Root morphology and biomechanical characteristics of high altitude alpine plant species and their potential application in soil stabilization

C. Hudek[1,2*], C. J. Sturrock[3], B. S. Atkinson[3], S. Stanchi[1], M. Freppaz[1]

[1]University of Torino, DISAFA, Largo Paolo Braccini, 2, 10095 Grugliasco (TO), Italy

[2]T2M, Marie Curie Cofund Fellow

[3]Hounsfield Facility, School of Biosciences, The University of Nottingham, Sutton Bonington Campus, Nr Loughborough, LE12 5RD, UK

*chudek@unito.it

Abstract

Glacial forefields host young, poorly developed soils with highly unstable environmental conditions. Root system contribution to soil stabilization is a well-known phenomenon. Identifying the functional traits and root morphology of pioneer vegetation that establish on forefields can lead us to useful information regarding the practical application of plants in land restoration of high altitude mountain sites.

This study aims to gather information on the root morphology and biomechanical characteristics of the 10 most dominant pioneer plant species of the forefield of Lys Glacier (NW Italian Alps).

X-ray Computed Tomography (X-ray CT) was used to visualize and quantify non-destructively the root architecture of the studied species. Samples were cored directly from the forefield. Data on root traits such as total root length, rooting depth, root diameter, root length density and number of roots in relation to diameter classes

as well as plant height were determined and compared between species. Roots were also tested for their tensile strength resistance.

X-ray CT technology allowed us to visualize the 3D root architecture of species intact in their natural soil system. X-ray CT technology provided a visual representation of root–soil interface and information on the exact position, orientation and elongation of the root system in the soil core. Root architecture showed high variability among the studied species. For all species the majority of roots consisted of roots smaller than 0.5 mm in diameter. There were also considerable differences found in root diameter and total root length although these were not statistically significant. However, significant differences were found in rooting depth, root length density, plant height and root tensile strength between species and life forms (dwarf shrub, forb, graminoid). In all cases root tensile strength decreased with increasing root diameter. The highest tensile strength was recorded for graminoids such as *Luzula spicata* (L.) DC. and *Poa laxa* Haenke and the lowest for *Epilobium fleischeri* Hochst. The differences in root properties among the studied species highlight the diverse adaptive and survival strategies plants employ to establish on and thrive in the harsh and unstable soil conditions of a glacier forefield. The data determined and discovered in this study could provide a significant contribution to a database that allow those who are working in land restoration and preservation of high altitude mountain sites to employ native species in a more efficient, effective and informed manner.

Keywords: alpine species; glacier forefield; root phenotyping; soil stabilization; X-ray CT

1. Introduction

Glaciers in alpine regions are affected by climate change twice as much as the global average with respect to other ecosystems (Bradley et al., 2014) which results in accelerated glacial retreat. Retreating glaciers expose young soils that are low in nutrients (carbon and nitrogen) (Bradley et al., 2014; Lazzaro et al., 2010) and highly unstable (Matthews, 1999). Mass wasting and erosion processes are common in these forefields creating an inhospitable environment for plant colonization (Siomos, 2009). Vegetation establishment on glacier forefields requires species with strong adaptive strategies and with high stress and disturbance tolerances (Robbins and Matthews, 2009). In spite of the harsh environment, vegetation cover increases quickly (Matthews, 1999) due to the rapid colonization of pioneer species. Pioneer species can grow quickly on nitrogen poor soils due to their high reproduction capacity and photosynthetic activity, (Stöcklin and Bäumler, 1996) and tolerance against abiotic stresses e.g., extreme temperatures, ultraviolet radiation, atmospheric pressure, shortage of mineral nutrients (Jones and Henry, 2003 Körner, 2003; Stöcklin et al., 2009).

Successful colonization and establishment of alpine species on glacial forefields may provide important information on the practical aspects of land reclamation and habitat restoration (Robbins and Matthews, 2009). Root traits (architectural, morphological, physiological and biotic) play an important role in both the physical and, even though the present study will not discuss further, also the chemical development of young soils (Bardgett et al., 2014; Massaccesi et al., 2015) bringing about increased structural stability in the forefield (Bardgett et al.,2014) and

decreasing the frequency and severity of any mass wasting and erosion processes. The biomechanical characteristics of roots such as tensile strength is a useful parameter for the quantification of the reinforcement potential; in particular for quantifying the added soil cohesion provided by plant roots. Determining the tensile strength of roots and their distribution in the soil profile can provide information on the increased shear strength of the soil provided by root reinforcement which can also determine plants' resilience to solifluction, frequently occurring in a periglacial environment (Jonasson and Callaghan, 1992). Quantitative data on root traits and architecture is one of the most significant variables considered when plants are evaluated for soil stabilization (Stokes et al., 2009). However data on root traits of alpine species remains scarce (Hu et al., 2013; Jonasson and Callaghan, 1992; Nagelmüller et al., 2016; Onipchenko 2014; Pohl et al., 2011; Zoller and Lenzin, 2006) which limits our understanding of the role these plants can play in root-soil interactions on the forefield.

Traditional techniques applied to examine the root system such as rhizotron or mini rhizotron, the use of paper pouches, synthetic soil media are all limited by the visual tracking of roots and/or creating an artificial environment that can lead to distorted/deceptive results. Destructive root phenotyping methods can also produce misleading results (Mooney et al., 2012) as they involve the separation of roots from the soil media meaning the relationship of the roots to the soil and to each other can no longer be observed (Pierrer et al., 2005). Additionally, repeated analysis on the same root system over time cannot be carried out e.g., dynamics of root growth or derivation of root demography (Koebernick et al., 2014).

Non-destructive imaging techniques such as Neutron Radiography, Magnetic Resonance Imaging (MRI) and X-ray Computed Tomography (X-ray CT) have been

effectively used in root phenotyping as they overcome the limitations of traditional techniques and are able to provide results on intact root systems in undisturbed soil. Research involving modeling (e.g., Water Erosion Prediction Project (WEPP) or Chemicals, Runoff and Erosion from Agricultural Management Systems (CREAMS)) also benefits from the enhanced quality of numerical data on root traits provided by these state of the art techniques (Lobet et al., 2015; Tasser and Tappeiner, 2005).

X-ray CT has already been successfully employed in many studies focusing on plant roots (e.g., Aravena et al., 2011; Mooney et al., 2006; Pierret et al., 1999; Wantanabe et al., 1992) to obtain clear, 3D images of intact root systems in the soil without the paramagnetic (Materials that are attracted by an externally applied magnetic field and form internal, induced magnetic fields in the direction of the applied magnetic field. (Boundless, 2016)) impact on the image quality found in MRI (Mooney et al., 2012; Koebernick et al., 2014). Whilst the majority of X-ray CT studies have been carried out on agricultural species such as wheat (Jenneson et al., 1999; Gregory et al., 2003; Mooney et al., 2006), maize (Lontoc-Roy et al., 2006), soybean (Tollner et al., 1994), potato (Han et al., 2008) and tomato (Tracy et al., 2012), a few studies can be found on tree roots (Pierret et al., 1999; Kaestner et al., 2006; Paya et al., 2015) and grasses (Pfeifer et al., 2015). As yet, no research has been carried out on the root architecture of alpine species under natural soil conditions using the X-ray CT.

In the majority of these studies, sieved, pre-prepared, organic matter-poor soils were used as the plant growth matrix, as the greater amount of organic particles can make root differentiation from soil particles more difficult, hampering root segmentation (i.e. the process of partitioning a digital image into multiple segments). Moreover, the

moisture distribution within undisturbed soil is more inconsistent which may also complicate the image segmentation process due to variations in image grayscale range of the roots under investigation (Pfeifer et al., 2015). While there have been a number of studies on the relationship between the natural soil matrix and the roots that permeate it, these studies have tended to focus on aspects of soil architecture rather than the architecture of the root (e.g., soil macropores, soil pore space) (e.g., Hu et al., 2016; Kuka et al., 2013).

The aim of the present study is to investigate and compare the root architecture and root traits of the ten most dominant pioneer plant species of the forefield of Lys Glacier (NW Italian Alps) in their natural soil system by producing accurate 3D images of their root system using X-ray CT. The value of the X-ray CT is verified by comparing the obtained results with other commonly employed techniques. Moreover, root tensile strength measurements will be made to understand the biomechanical role of the plant species on soil stabilisation. The retrieved information is discussed in the light of the potential future use of the studied species for slope soil reinforcement.

2. Materials and methods

2.1 Study site

Plant sampling was carried out on the recently deglaciated forefield of the Lys Glacier in the Aosta Valley (North West Italy). The glacial till was deposited in 2004

at an altitude of 2300 m above sea level on a bedrock of granitic gneiss and paragneiss belonging to the Monte Rosa nappe (D'Amico et al., 2014). The climate is alpine subatlantic with a mean annual rainfall of 1200 mm. The mean annual air temperature is -1 °C (Mercalli, 2003) with a winter temperature below -4 °C on average. The sampling site is south facing with a soil texture of loamy sand and an udic moisture regime (Soil Survey Staff, 2010). The chemical properties of the soil at the study site correspond to a slightly acidic soil (pH 5.8 - 6.7) with very low amounts of total nitrogen (TN) and total organic carbon (TOC) (0.002-0.017 g kg^{-1} and 0.018-0.217 g kg^{-1} respectively) with available phosphorus (P) of 1.3-4.7 mg kg^{-1} (Hudek et al., 2017). Pioneer alpine plants, mostly graminoid and forb species colonize the site (e.g., *Epilobium fleischeri* Hochst., *Linaria alpina* (L.) Mill., *Trisetum distichophyllum* (Vill.) P. Beauve.), a detailed vegetation survey of the moraine can be found in D'Amico et al. (2014).

2.2 Sampling approach

The ten most common plant species of the forefield were selected. These were sampled between August and September 2015; *E. fleischeri*, *T. distichophyllum*, *Trifolium pallescens* Schreb., *Luzula spicata* (L.) DC., *Silene exscapa* All., *Minuartia recurva* (All.) Schinz and Thell., *Festuca halleri* All. *Poa laxa* Haenke, *Salix helvetica* Vill. and *Leucanthemopsis alpina* (L.) Heyw (Table1). A total of 60 soil columns, (i.e. 6 columns per species) were excavated. During sampling, special care was taken to avoid individuals with any visible neighbouring plant effects (Gaudet and Keddy, 1988) and to keep plant size as equal as possible for all 60 samples. One sample from each species was cored 10 samples in total) with their own PVC cylinder

(maximum sample height of 20 cm x diameter of 7.4 cm). After coring, the ten soil columns were carefully secured and placed in plastic bags and transported to the laboratory. In the laboratory the cored samples were placed in a climate chamber until the X-ray CT tests were undertaken. The climate chamber was set to provide conditions so as to delay root decay using a photoperiod of 14 hours, a relative humidity of 65 % and temperatures of 15 °C by day and 10 °C by night.

The remaining five replicates of each species (a total of 50) were excavated with a trowel. The 50 soil columns containing the root system of the individuals were placed in plastic bags, transported to the laboratory and stored at 3.5 °C until measurements were undertaken (Bast et al., 2015).

Table 1 The selected 10 pioneer plant species of the forefield of Lys Glacier according to their Latin and common names, lifeforms, succession and family.

Species	Common name	Life form	Succession	Family
Epilobium fleischeri Hochst.	Alpine willowherb	Forb	Early	Omagraceae
Trisetum distichophyllum (Vill.) P.Beauve.	Tufted hairgrass	Graminoid	Early	Poaceae
Trifolium pallescens Schreb.	Pale clover	Forb	Early	Fabaceae
Luzula spicata (L.) DC.	Spiked woodrush	Graminoid	Mid	Juncaceae
Silene exscapa All.	Moss campion	Forb	Mid	Caryophyllaceae
Minuartia recurva (All.) Schinz and Thell.	Recurved sandwort	Forb	Late	Caryophyllaceae
Festuca halleri All.	Haller's Fescue	Graminoid	Late	Poaceae
Poa laxa Haenke	Banff Bluegrass	Graminoid	Ubiquitous	Poaceae
Salix helvetica Vill.	Swiss willow	Dwarf shrub	Ubiquitous	Salicaceae
Leucanthemopsis alpina (L.) Heyw.	Alpine Moon Daisy	Forb	Ubiquitous	Asteraceae

2.3 Non-destructive root phenotyping

The cored samples from the PVC cylinder were scanned using a Phoenix V|TOME|X M 240 high resolution X-ray CT system (GE Sensing and Inspection Technologies, Wunstorf, Germany). The scanning parameters (Table 2) were optimized to allow balance between a large field of view and a high resolution. Due to the height of the

cylinder (20 cm) two separate scans (upper and lower part of the sample) were made to cover and image the entire sample. Each sub-scan was then reconstructed using DatosRec software (GE Sensing and Inspection Technologies, Wunstorf, Germany) and then manually combined in VG Studio MAX v2.2 (Volume Graphics GmbH, Heidelberg, Germany) and exported as a single 3D volumetric dataset. To distinguish the root system from the soil material image processing techniques were applied. Roots were segmented from the reconstructed CT data by using the region growing method (Gregory et al., 2003) in VG Studio MAX v2.2. Quantification of 3D root traits was undertaken using RooTrak software (Mairhofer et al., 2012). RooTrak was able to provide quantitative data on the root volume (total mass of the root system; mm^3), root area (root area in direct contact with the soil; mm^2), the root system's maximum vertical and horizontal length (mm) as well as the convex hull (the region of soil explored by the root system; mm^3) (Mairhofer et al., 2015).

Table 1 Scanning parameters for X-ray CT.

2.4 Destructive root phenotyping

Following X-ray CT scanning, the roots were extracted from the soil column by carefully cleaning the soil matrix from the roots with a water jet under a sieve mesh to retain remnants of roots that may come loose during the cleaning process. The washed roots were then placed into a 15 % ethanol solution and stored at 3.5 ºC. Then the root systems were scanned with a flatbed scanner (EPSON Expression 11000XL). The images from scanning had a 600 dpi resolution and were used for two dimensional image analysis. This was with the aim to compare the CT scanned

219 results with the results of a, traditional technique (Paez-Garcia et al., 2015). Root
220 traits such as total root length, average root diameter, and the root system's
221 maximum vertical and horizontal length were considered for analysis.
222 The remaining 50 plant samples (five replicates of each species were followed the
223 same cleaning, storing and scanning method as before . All 2D scanned images
224 were analyzed with the WinRHIZO 2013e and ImageJ software. The data collected
225 on root traits were total root length, root length distribution (%) in different diameter
226 classes, average root diameter, root length density, rooting depth and total plant
227 height. Additionally plant height was measured according to the standardized
228 measurement of plant functional traits (Pérez-Harguindeguy et al., 2013).
229
230 2.5 Root tensile strength
231
232 Root tensile strength tests were performed to determine root resistance to breaking
233 under tension (Bischetti et al., 2005; Pohl et al., 2011). The complete root system,
234 kept in a 15 % ethanol solution was first cut into individual root segments. Randomly
235 selected undamaged roots with the widest available range of diameters were then
236 selected for testing. Before testing, root diameter at three points of the root segment
237 were measured with a digital caliper to obtain the average root diameter of the
238 individual root sample. This is necessary as the exact position of root rupture is
239 unknown before testing.
240 Root tensile strength were measured in the laboratory using an electromechanical
241 universal testing machine, MTS Criterion, Model 43 (MTS Systems, Eden Prairie,
242 MN, USA). Plant roots were secured between clamps at both ends. The clamps
243 consist of two metal discs (washers) covered with drafting tape holding the roots in

244 place. The speed reduction of the device was maintained at a steady 10 mm min^{-1} as
245 it was suggested in other studies (Bischetti et al., 2005; Bordoni et al., 2016; De
246 Baets et al., 2008; Yang et al., 2016) and the tensile force was measured by a load
247 cell (500N) connected to a computer to record the results. Roots broke when they
248 could no longer resist tensile force. Measurement results were excluded from data
249 analysis when root rupture occurred near the clamp. Measurement was considered
250 to be successful when the rupture occurred in the middle of the root section
251
252 2.6 Statistical analysis
253
254 In the present study comparative data analysis on root traits between the non-
255 destructive and destructive technique was only respected when comparing the
256 maximum vertical and horizontal length of the root system due to the lack of data
257 available on very fine roots (< 0.5 mm) on the 3D images.
258 Results obtained from X-ray CT scanning (RooTrak) on the root system's maximum
259 vertical and the maximum horizontal length were compared with results obtained
260 from the destructive method (ImageJ) by applying Pearson's correlation test. Once
261 the normality and homogeneity of variance were verified a one-way analysis of
262 variance (ANOVA) was used to detect differences in the measured root properties
263 (root length density, total root length, mean root diameter, rooting depth, root length
264 distribution within diameter classes) and plant height among the studied species. In
265 cases when significant differences were found between the groups, the Tukey post
266 hoc test was run to detect where the differences occurred between the groups.
267 The relationship between root tensile strength and root diameter was evaluated by
268 fitting a regression curve (power law equation). Analysis of covariance (ANCOVA)

was performed to compare tensile strength results between the 10 studied species and to take root diameter into consideration as a covariant. Both tensile strength and root diameter values were log transformed before the analysis. All assumptions were tested before carrying out ANCOVA (linearity, homogeneity and normality). All statistical analysis was carried out using the statistical software SPSS Statistics 22 (IBM SPSS, 2013).

3. Results

3.1 Non-destructive root phenotyping

X-ray CT was successfully used to reveal the 3D root architecture of the studied 10 species. Tap roots and thicker lateral roots (diameter >0.5 mm) were identified in all cases while individual examples of thinner lateral roots (diameter < 0.5 mm) were only identified for *S. helvetica*, *P. laxa*, *L. spicata* and *F. halleri,* (diameters of 0.35, 0.35, 0.25 and 0.25 mm, respectively). Even though it was not possible to extract the entire root system, a visual representation of root–soil contact in the undisturbed position, orientation and elongation of the core root system was possible. It should be noted that due to the size limitation of the PVC cylinder and the difficulty of identifying root position when coring, the tap root and/or lateral roots were cut off by the edge of the cylinder therefore the max vertical and horizontal root length in the present study is approximate and should only be taken into consideration as part of data validation for RooTrak.

The maximum vertical and horizontal root length data obtained from the 3D images were underestimated by an average of 42% and overestimated by 26% respectively

when compared to measured data with ImageJ. The results from the Pearson's correlation tests between RooTrak and ImageJ showed a week positive correlation (r= 0.57, p=0.084) for maximum vertical root length and a very week negative correlation (r= -0.38, p=0.275) for the maximum horizontal root length (Figure 3b). Because the p-values are non-significant at the p=0.05 level, there is inconclusive evidence about the association between the variables.

The highest root volume, root area and convex hull (Table 3) were all recorded for *T. pallescens* (1530 mm^3, 7752 mm^2, 505384 mm^3 respectively). The lowest root volume was recorded for *M. recurva* and *P. laxa* (144 and 150 mm^3 respectively) while the lowest value of root area (1146, 1547 and 1677 mm^2) and convex hull (24117, 45612, 60237 mm^3) was recorded for *S. helvetica, P. laxa* and *M. recurva* respectively. Results from *F. halleri* and *L. spicata* were excluded from the comparison as it was difficult to identify and segment the high number of fine (< 0.25 mm), overlapping roots and in many cases it was not possible at all. Therefore including the results of *F. halleri* and *L. spicata* would have caused misleading overall results.

Table 3. Values of root traits analyzed with RooTrak (volume, area, maximum vertical and horizontal length of the root system, convex hull), ImageJ (maximum

318 vertical and horizontal length of the root system) and WinRHIZO (total root length
319 and average root diameter) of the X-ray CT scanned samples.
320
321 The highest total root length (roots 0.1-0.5 mm in diameter) was recorded for *T.*
322 *distichophyllum*, *L. spicata* and *S. exscapa* (192.7, 100.3 and 95.3 m respectively)
323 and the lowest for *P. laxa* and *F. halleri* (10.5 and 20.7 m respectively). The rest of
324 the species results fell between the values of 50.5 and 62.2 m (Table 3).
325
326 Average root diameter ranged between 0.16 and 0.31 mm. The lowest root
327 diameters were recorded for *L. spicata* and *E. fleischeri* (0.16 mm and 0.17 mm
328 respectively) and the highest for *F helleri* and *T. pallescens* (0.31 mm and 0.30 mm
329 respectively) (Table 3).
330
331 **Figure 3** *a.,* Linear relationship between RooTrak and ImageJ data on the maximum
332 vertical and *b.,* horizontal root length for the 10 studied alpine species.
333 The overall root architecture for each species displayed considerable variation
334 (Figure 1 a-j). To determine and differentiate root system architecture between the
335 species the root type classification established by Lichtenegger and Kutschera,
336 (1991) was applied:
337 *E. fleischeri* showed a dominant pole root system with strong horizontal root
338 spreading indicating the intense clonal growth of the plant. *T. pallescens* showed a
339 cone shape and *S. exscapa* a wider cone shape upward extended root type. *S.*
340 *helvetica* and *M. recurva* had a discoid shaped root system due to the shallow depth
341 of rooting but large lateral spreading. *P. laxa*, *F. halleri* and *L. spicata* all showed a

cone shape downwards dilated root type while *L. alpine* had an umbrella shaped and *T. distichophyllum* a cylindrical shaped root type.

Figure1. Root architecture of the 10 studied pioneer alpine species detected by X-ray CT scanning. Scale bars: a., 35 mm, b., 25 mm, c., 40 mm, d., 15 mm, e., 10 mm, f., 15 mm, g., 15 mm, h., 30 mm, i., 45 mm, j., 20 mm.

Figure 2 *a.,* Image of the core root system *b.,* the core root system in relation to the soil matrix and *c.,* the washed entire root system of *T. pallescens*. Scale bar a., 45 mm b., 40 mm and c., the ruler uses cm.

The natural soil matrix showed a great variation in terms of soil structure among the cored samples. Figure 5 a-c shows examples of the structural diversity of the samples. The soil matrix in Figure 5 a., indicates a deposition of glacial till with little reorganization due to slope processes as Figure 5 b., and c., are fluvio-glacial and lake depositions with visible silt and sand layers.

Figure 5 Examples of the grayscale CT images of the soil matrices *a.,* glacial till with *T. distichophyllum b.,* and *c.,* fluvio-glacial and lake depositions.

3.2 Destructive root phenotyping

Root length density results (Table 4) varied greatly among the studied species (9–85 cm cm^{-3}). The lowest density was recorded for *E. fleisheri*, *M. recurva* and *T. pallescens*, with 9 29 and 33 cm cm^{-3} respectively and the highest was recorded for

T. distichophyllum and *L. spicata* with 85 and 81 cm cm^{-3} respectively. There was significant difference found in root length density among the species (F (9, 22) = 4.78, p <0.001). Post-hoc comparisons using the Tukey HSD test indicated that root length density differed significantly (p <0.05) between *E. fleisheri* and *L. spicata*, *T. distichophyllum*, *S. helvetica* and *F. halleri* as well as between *M. recurva* and *L. spicata*. There was no statistically significant difference in root length density between the other species. However, the difference between *T. pallescens* and *L. spicata* showed a substantial trend toward significance (p=0.078) as well as between *M. recurva* and *T. distichophyllum* (p=0.062). Specifically, the results suggest that out of the ten studied species, only *E. fleisheri's* and *M. recurva's* root system resulted in a significantly lower root length density when compared to the majority of the studied plants. It should be noted that in most but not all cases, higher root length density was found among the graminoid (*L. spicata, T. distichophyllum, F. halleri*) and the dwarf shrub (*S. helvetica*) species.

Commented [SS1]: Why not putting letters in table? As it is looks difficult to read…

Total root length results (Table 4) showed no significant differences between the species (F (9, 39) =1.07, p=0.417) even though the mean results showed moderate variability among them (75.3–368.5 m). The shortest length was recorded for *E. fleischeri*, and *S. exscapa*, with 75.3 and 106.2 m respectively and the highest for *L. alpina* and *S. helvetica* with 368.5 and 342.3 m respectively.

Table 4 Plant height (mm), rooting depth (mm) measured with ImageJ, total root length (m), mean root diameter (mm) and root length density (cm cm-3) of the 10 studied alpine species measured with WinRhizo.

392 Table 5 shows the root length distribution in different diameter classes (%). Eight out
393 of ten species had their highest root count (57-36 %) in the diameter class 0<L<=0.1
394 mm with the exception of *T. distichophyllum* and *S. helvetica* which had it at
395 0.1<L<=0.2 (41 %) and 0.2<L<=0.3 mm (37 %) respectively. *T. pallescens* and *S.*
396 *helvetica* also had roots larger than 2 mm in diameter as the other species rarely
397 exceeded 1 mm in diameter.
398
399 **Table 5** Root length distribution (%) of the 10 pioneer alpine plants in relation to
400 different diameter classes (mm).
401
402 **Figure 4** Root length distribution (%) in relation to root diameter classes (mm) for the
403 10 studied alpine species
404
405 The mean root diameter results (Table 3) also showed no significant differences
406 between the species (F (9, 22) =1.78, p=0.129) values. The results ranged between
407 0.21 mm and 0.47 mm. The lowest mean root diameter was recorded for *T.*
408 *distichophyllum* with 0.21 mm and the highest for *T. pallescens* with 0.47 mm.
409
410 Rooting depth results (Figure 6), determined by ImageJ showed considerable
411 variation among the species, ranging from 9 to 19.7 cm. The deepest penetrating
412 root system was recorded for *E. fleischeri* and the shallowest for *S. helvetica*. A one-
413 way ANOVA was used to compare the rooting depth results (Table 4) between the
414 10 species which showed significant difference at F (9, 38) = 2.38, p <0.03. The
415 Tukey HSD test indicated that *E. fleischeri* had a significantly longer rooting depth
416 than *S. helvetica* and *F. halleri*.

Commented [SS2]: Insert letters in table 4

Plant height also varied between the species, ranging from 15 to 65 cm (Table 4). The highest plant height was recorded for *E. fleischeri* (65 mm) and the lowest for *M. recurva* (15 mm). There was significant difference found at F (9, 29) = 57.73, P< 0.001) between the studied species.

Figure 6 Plant height (cm) and rooting depth (cm) of the 10 studied alpine plant species.

3.3 Root tensile strength

There was a great variation in the tensile strength results among the studied species (Table 6). The highest mean tensile strength was found at the graminoid and shrub species ranging between 138-86 MPa and the lowest among the forbs ranging between 60-29 MPa. The results showed that graminoid species have comparable tensile strength results to the dwarf shrub *S. helvetica*. When the significant differences were tested between the studied species taking root diameter into consideration as a covariate the results showed significant differences between the studied species at F (8, 256) =8.338, p<0,001. In all cases the assumptions, homogeneity and normality were satisfied, except for one case *E. fleischeri* for which the variances were non-homogeneous. Therefor *E. fleischeri* was excluded from the comparison. The corrected mean values indicate the resistance ranking of species with decreasing order: *P. laxa, F. halleri, T. distichophyllum, S. helvetica, T. pallescens, S. exscapa, L. spicata, M. recurva, L. alpine*.

441 Tensile strength and the related root diameter values were plotted (Figure 7) to show
442 the relationship between root tensile strength and root diameter which confirmed the
443 power law relationship meaning that with increasing root diameter root tensile
444 strength decreased.
445
446 **Table 6** Life forms, the number of samples (n) tested, the range of root diameters
447 (mm), root tensile strength (MPa) values, scale factor (α) rate of strength decrease
448 (β) and the goodness of fit (R^2) of the 10 studied alpine species.
449
450 **Table 7** ANOVA table with multiple comparisons of root tensile strength (MPa)
451 between the studied plant species.
452
453 **Figure 7** The relationship between root tensile strength (MPa) and root diameter
454 (mm) for the 10 studied alpine species
455
456
457 **4. Discussion**
458
459 4.1 Non-destructive root phenotyping
460
461 The X-ray CT scanning has provided the first ever 3D images of the intact core root
462 system of 10 different pioneer alpine plant species in their natural soil matrix. Visual
463 information on the vertical and horizontal spreading as well as the rooting angle and
464 branching of thicker roots in connection to the soil matrix were visible and could be
465 important information when determining the significance of the root system on soil

466 reinforcement in future studies (e.g. the resistance of the root system to uprooting or
467 its protective role against shallow landsliding). During the use of X-ray CT several
468 challenges and limitations were discovered; Some aspects made it difficult to decide
469 on the scanning parameters. There was a limited amount (Stöckli and Bäumler,
470 1996; Pohl et al., 2011) or no data available on the root traits of the studied species
471 prior to testing. They also had varying characteristics in terms of life form, family
472 (Körner, 2003; Pignatti, 2003; Broglio and Poggio, 2008) and succession (Damico et
473 al., 2014; Stöcklin and Bäumler, 1996) indicating different root architecture and
474 anatomy. Additionally they had never been subject to study with current state of the
475 art phenotyping techniques. The samples were cored from their natural habitat in a
476 heterogenic soil matrix and the soil absorbed a high level of the X-rays resulting in
477 prohibitively long scans to achieve the necessary beam penetration. The tracking of
478 individual roots during segmentation was extremely difficult as the heterogenic soil
479 matrix made it difficult to differentiate roots from other organic particles in the soil
480 (Figure 4 a, b, and c). Additionally the root system contained vast amounts of
481 overlapping roots and neighbouring plant roots were invariably cored together with
482 the test sample even when, from the surface, samples appeared free from any
483 neighbouring plant effects.
484 Roots with a diameter >0.5 mm are visible on the 3D images. These thicker roots
485 allow us to estimate the location of thinner roots (Stokes et al., 2009). Not being able
486 to detect the thinner roots on the present 3D images was not due to the limitations of
487 the X-ray CT technology, rather the issue of resolution, sample size and the
488 heterogenic soil matrix. In general, in homogeneous background the minimum
489 resolution should be set twice as high as the cored sample is long in millimeters and
490 set even higher if the background is heterogenic (Kaestner et al., 2006). A higher

resolution setting however would have resulted in a prohibitively prolonged scanning and segmenting time. The method suggested by Kaestner et al. (2006) was successful at detecting roots with a diameter <0.5 mm in homogeneous background, however roots in heterogeneous soil matrix (Figure 4 a-c) remained challenging. Cored samples of reduced length and diameter may have allowed for the detection and segmentation of the finer roots within the system but the compromise would be the smaller PVC cylinders would not have been suitable for sampling the species from the field without causing damage i.e. preventing disturbed soil conditions within the sample. A factor to possibly bear in mind for future work conducted on alpine species with fine root systems would be to take two sets of cores when assessing the different scales in root architecture.

Interestingly, although it was not possible to segment using the available software; many of the fine roots were often visible to the naked eye when manually scrolling through the greyscale images providing a unique insight into the complexity of these alpine species.

4.2. Analysis of root architecture and root traits

S. exscapa and *T. pallescens* both have a dominant tap root morphology with a large number of tillers. Their tap root and thicker lateral roots are often found growing through cracks in the bedrock thereby anchoring the plant and stabilizing the soil from shallow landsliding. The number of lateral roots and the diversity of their branching angles resulting in a larger shear zone indicate an increased soil stability (Abe and Ziemer, 1991). Both *S. exscapa* and *T. pallescens* have dense, fine root

networks that can play an important role in reducing soil erosion. Root nodules are clearly visible on the roots of *T. pallescens* reflecting the existing association the plant has with symbiotic nitrogen-fixing bacteria (Holzmann and Haselwandter, 1988).

S. helvetica also has a dominant taproot morphology with the potential of growing through cracks in the bedrock though it has a shallower rooting depth than *S. exscapa* or *T. pallescens*. *S. helvetica* has a large lateral spread in the upper soil layer with a dense fine root network which can provide increased support in soil erosion control and horizontal anchoring.

The uniform length of the umbrella shaped root system of *L. alpina* could be easily uprooted therefore, its potential as soil reinforcement might be limited although it is capable of trapping a significant amount of soil due to its dense fine root network (Hudek et al., 2017) and reducing soil erosion.

The dominant pole type of root system of *E. fleischeri* showed the greatest rooting depth with intensive rhizome spreading. The main feature of the plant's strategy is rapid colonization of open space through wide lateral clonal spreading (Stöckli and Bäumler, 1996) which is a typical strategy for early successional plants such as *Hieracium staticifolium* All*., Achillea moschata* (Wulfen) or *Cerastium pedunculatum* Gaudin (Stöckli and Bäumler, 1996). Its root system does not have notable anchoring properties, its survival strategy relies on an elaborate network of rhizome spreading, widely spaced ramets and rapid colonization (Alpandino, 2011). In this way the plant is able to quickly overcome diverse mass wasting processes. Additionally its short and fragile fine root (<1mm) network is unclearly able to provide additional soil stabilization (Bischetti et al., 2009) even though plant biomass and allometry are stated being a significant element when plants are evaluated for soil-

541 root reinforcement (Gonzalez-Ollauri and Mickovski, 2016). In general the function of
542 these roots is limited to water and nutrient uptake to support plant growth (Stokes et
543 al., 2009; Tasser and Tappeiner, 2005).
544 *T. distichofillum* also uses horizontal spreading through clonal growth as a strategy
545 for rapid colonization but with shorter distance between ramets (Alpandino, 2011). It
546 also has a dense lateral root system with moderate rooting depth and a high
547 percentage of fine and very fine roots throughout the entire root system. This can
548 make the plant more resilient to uprooting and at the same time, through the
549 elaborate network of rhizome spreading, able to overcome diverse mass wasting
550 processes (Körner, 2003). Its dense fine and very fine roots trap soil providing
551 erosion control. *P. laxa* is a plant with clumped clonal growth form with short distance
552 between ramets. *F. halleri* and *L. spicata* both form compact tussocks with a dense
553 fibrous root system. This phalanx type of clonal growth results in a slow horizontal
554 spreading (Alpandino, 2011). These types of root morphology can make the plants
555 extremely resilient to uprooting and a potentially effective plant in erosion control.
556 The root architecture of the species showed a wide range of root types dictated by
557 genetic characteristics (Gray and Sotir, 1996) and environmental factors e.g.,
558 nutrient availability or soil temperature (Nagelmüller et al., 2016; Khan et al., 2016).
559 Root plasticity too has effects on root architecture, it is essential in coping with and
560 overcoming stress (Bardgett et al., 2014; Poorter et al., 2012; Stöcklin and Bäumler,
561 1996) as well as strengthening the resilience of pioneer species to the harsh
562 environmental conditions.
563 Even though *E. fleischeri* had a significantly higher rooting depth compared to the
564 other species, in general, rooting depth was uniformly shallow which is in line with
565 previous findings (Lichtenegger, 1996; Jonasson and Callaghan, 1992; Pohl et al.,

2011) on alpine species. This is influenced by two main controlling environmental factors; soil temperature and water availability (Lichtenegger, 1996; Körner, 2003). Alpine vegetation in general have a shallower rooting system than species from lowlands as at high altitudes with increasing soil depth, soil temperature and water fluctuations decrease at a higher rate than in the lowlands (Lichtenegger, 1996). This also can reflect on root distribution within the different soil horizons, indicating that the high root density in the upper soil layer quickly decreases with increasing soil depth (Lichtenegger, 1996).

Root length density has a great influence on soil stability (Bardgett et al., 2014; Stokes et al., 2009) by altering the hydrological properties of the soil and increasing the resistance of the roots for disruptive forces. All studied species had a large amount of fine and very fine roots which is common in alpine species (Körner, 2003; Pohl et al., 2011). In general, fine and very fine roots have a rapid turnover supplying a large amount of carbon to the soil and increasing the organic content of the soil. Together with the physical and chemical contribution they gradually increase the aggregate stability of the soil which reduces the susceptibility of the soil to erosion processes (Pohl et al., 2011; Hudek et al., 2017). Additionally, both live and dead roots provide potential preferential flow paths in hillslopes, securing the stability of the soil by reducing pore water pressure (Ghestem et al., 2011). On the other hand, bypass flow can lead to perched water tables, saturating the soil that can develop positive pore-water pressure that could trigger landslides (Ghestem et al., 2011). Glacier forefields are nutrient limited soils; fine and very fine roots (< 0.5 mm) however, provide strong symbiotic links between the plant and the fungus systems and it has been proven that mycorrhizal fungi increases the water and nutrient uptake of the plant (Smith and Read, 2008) and promote root growth (Ola et al.,

591 2015) which also influences RLD (Bast et al., 2014; Graf and Frei 2013; Tisdall,
592 1991). The dense fine root system of the studied species is also able to mechanically
593 bind the soil particles thereby contributing to increased soil stabilization (Pohl et al.,
594 2011; Norris et al., 2008).
595 In the present study the total root length values showed non-significant difference
596 between the species and life forms while the highest values were recorded among
597 the graminoid species as was with the work of Pohl et al. (2011) though in the
598 present study the measured values greatly exceed those of Pohl et al. (2011). This
599 can be attributed to the fact that at the sampling site of Pohl et al., (2011) sampling
600 was carried out on managed ski slopes where soil compaction inhibits root growth
601 (Nagel et al., 2012; Pfeifer et al., 2014) while in the case of our study on the recently
602 deglaciated forefield, sampling was performed on a site relatively free from human
603 interference and soil compaction was not an inhibiting factor for root growth.
604 Under natural conditions species grow together creating a complex underground root
605 network/structure due to the diversity of root types, enlarging the protective role of
606 plants on soil stabilization at different levels and soil layers (Pohl et al., 2009;
607 Reubens et al., 2007). Plant richness should therefore be encouraged when plants
608 are considered for soil conservation purposes such as land reclamation.
609
610 4.3. Root tensile strength
611
612 The tensile strength results of the present study were 3-7 times higher than those
613 found in literature data on the same alpine species (*L. spicata, L.alpina*) (Pohl et al.,
614 2011) and other alpine and arctic graminoid and forb species (Pohl et al., 2011,
615 Jonasson and Callaghan, 1992). Root tensile strength is mainly effected by the

genetic properties of the plant (Gray and Sotir, 1996) while additional factors such as age (Reubens et al, 2007), ecological conditions and management practices(Bischetti et al., 2009) can result in varying tensile strength values for the same species. Gonzallez-Ollauri et al. (2017) highlighted that root tensile strength can vary with changes in root moisture content which closely links to soil moisture content (i.e. dry roots have a lower level of tensile strength compare to roots with optimum root moisture). Root diameter has direct influence on root tensile strength as root tensile strength is calculated by the ratio between the breaking force (N) and the root cross section area (mm^2) which depends on root diameter (Bischetti et al., 2016). In general, fine and medium size roots (in diameter 0.01-10.00 mm) have higher values of tensile strength compared to roots with a larger diameter (> 10.00 mm). Larger sized roots act primarily as individual anchors mobilising only a small amount of their tensile strength before slipping through the soil (Bischetti et al., 2005). However, fine and medium sized roots can mobilize their entire tensile strength and due to their higher surface area, have superior resistance to uprooting (Gray and Sotir, 1996). In the present study the diameter of the tested roots ranged between 0.03 mm and 1.66 mm, these values are smaller than what is found in the literature data which can be one of the explanation for the considerably higher tensile strength results. Additionally the samples in Pohl et al. (2011) were collected from a managed ski slope which confirms results observed by Bischett et al. (2009) that ecological conditions and management can alter tensile strength.

Both the ANCOVA and the plotted tensile strength results enabled it to demonstrate the significant relationship between tensile strength and root diameter and can be used to make comparisons between species.

642 ## 5. Conclusions

643

644 This study aimed to provide information on root morphology and root traits on
645 pioneer alpine species from a recently deglaciated site in the Italian Alps with the
646 view to determine the plants' efficiency in soil stabilization. To provide unique visual
647 3D data on the root architecture of a wide variety of alpine pioneer species under
648 intact natural soil conditions, we applied a state of the art non-destructive plant
649 phenotyping technique, X-ray CT. This is the first study that uses the X-ray CT
650 technique to image the root system of alpine plants undisturbed in their natural
651 alpine soil matrix.
652 Results showed great variation in global root architecture between the studied
653 species. X-ray CT could successfully identify roots >0.25, 0.35 mm in diameter at the
654 resolution used for scanning. With complementary use of destructive phenotyping
655 techniques, quantitative data on root traits and the plants biomechanical
656 characteristic allowed us to determine species' efficiency in soil stabilization. The
657 high tensile strength results of graminoid and the dwarf shrub species combined with
658 a dense elaborate root morphology, provide many anchoring points and enhanced
659 plant resilience to solifluction in a periglacial environment. Forbs longer, anchoring
660 root system with lower but comparable tensile strength to the garminoid and dwarf
661 shrub species, could advocate their suitability as protection against shallow
662 landsliding. With the exception of one or two species (*E. fleischeri, M. recurva*) all
663 studied plants might play an important role in soil erosion control due to their dense
664 elaborate fine and very fine root system.

665

666

Commented [SS3]: Revise sentence it's difficult tot read...

667 **Acknowledgements**

668 This research was enabled by the Transnational Access capacities of the European
669 Plant Phenotyping Network (EPPN, grant agreement no. 284443) funded by the FP7
670 Research Infrastructures Programme of the European Union. As well as receiving
671 funding from the European Union's Horizon 2020 research and innovation
672 programme under the Marie Skłodowska-Curie grant agreement No 609402 - 2020
673 researchers: Train to Move (T2M). The Hounsfield Facility received funding from
674 European Research Council (Futureroots Project), Biotechnology and Biological
675 Sciences Research Council of the United Kingdom and The Wolfson Foundation.
676 The authors wish to thank Alessio Cislaghi, Enricho Chiaradia and Gian Battista
677 Bischetti for the access to and support with the tensile testing machine and Michele
678 Lonati for his help on the identification of graminoid species.

679

680 **References**

681

682 Abe, K., Ziemer, R.R., 1991. Effect of tree roots on a shear zone: modeling
683 reinforced shear stress. Canadian Journal of Forest Research 21, 1012-1019.
684 Alpandino, 2011. Alpandino by Institute of Botany, University of Basel, Switzerland.
685 https://www.alpandino.org
686 Aravena, J.E., Berli, M., Ghezzehei, T.A., Tyler, S.W., 2011. Effects of root-induced
687 compaction on rhizosphere hydraulic properties X-ray microtomography
688 imaging and numerical simulations. EnvSci & Tech, 45, 425–431.
689 Bardgett, R.D., Mommer, L., De Vries, F.T., 2014. Going underground: root traits as
690 drivers of ecosystem processes. Trends in Ecology and Evolution, 29, 12, 692-
691 699.

692 Bast, A., Wilcke, W., Graf, F., Lüscher, P., Gärtner, H., 2015. A simplified and rapid
693 technique to determine an aggregate stability coefficient in coarse-grained
694 soils. Catena, 127, 170-176.
695 Bischetti, G.B., Bassanelli, C., Chiaradia, E.A., Minotta, G., Vergani, C., 2016. The
696 effect of gap openings on soil reinforcement in two conifer stands in northern
697 Italy. Forest Ecology and Management, 359, 286–299.
698 Bischetti, G.B., Chiaradia, E.A., Epis, T., Morlotti, E., 2009. Root cohesion of forest
699 species in Italian Alps. Plant and Soil, 324, 71-89.
700 Bischetti, G.B., Chiaradia, E.A., Simonato, T., Speziali, B., Vitali, B., Vullo, P., Zocco,
701 A., 2005. Root strength and root area ratio of forest species in Lombardy
702 (Northern Italy). Plant and Soil, 278, 11–22
703 Bordoni, M., Meisina, C., Vercesi, A., Bischetti, G.B., Chiaradia, E.A., Vergani, C.,
704 Chersich, S., Valentino, R., Bittelli, M., Comolli, R., Persichillo,
705 M.G., Cislaghi, A., 2016. Quantifying the contribution of grapevine roots to
706 soil mechanical reinforcement in an area susceptible to shallow landslides.
707 Soil and Tillage, 163, pp. 195-206.
708 Boundless. “Diamagnetism and Paramagnetism.” *Boundless Chemistry* Boundless,
709 08 Aug. 2016. Retrieved 03 Mar. 2017.
710 https://www.boundless.com/chemistry/textbooks/boundless-chemistry-
711 textbook/periodic-properties-8/electron-configuration-68/diamagnetism-and-
712 paramagnetism-320-10520/
713 Bradley, J.A., Singarayer, J.S., Anesio, A.M., 2014. Microbial community dynamics in
714 the forefield of glaciers. Peoc. R. Soc.B 281: 20140882.
715
716 Broglio, M., Bovio, M., Poggio, L., 2008. Guida alla flora della Valle d'Aosta.

D'Amico, M.E., Freppaz, M., Filippa, G., Zanini, E., 2014. Vegetation influence on soil formation rate in a proglacial chronosequence (Lys Glacier, NW Italian Alps).CATENA, 113, 122-137.

Gaudet, C.L., Keddy, P.A., 1988. A comparative approach to predicting competitive ability from plant traits. Nature, 334, 242–3

Ghestem, M., Sidle, R.C., Stokes, A., 2011. The influence of plant root system on subsurface flow: Implications for slope stability. BioScience, 61, 869-879.

Gonzalez-Ollauri, A., Mickovski, S.B., 2016. Using the root spread information of pioneer plants to quantify their mitigation potential against shallow landslides and erosion in temperate humid climates. Ecological Engineering, 95, 302-315.

Gonzalez-Ollauri, A., Mickovski, S.B., 2017. Plant-soil reinforcement response under different soil hydrological regimes. Geoderma, 285, 141-150.

Gregory, P.J., Hutchinson, D.J., Read, D.B., Jenneson, P.M., Gilboy, W.B., Morton, E.J., 2003. Non-invasive imaging of roots with high resolution X-Ray micro-tomography. Plant Soil, 255, 351–359.

Graf, F., Frei, M., 2013. Soil aggregate stability related to soil density, root length, and mycorrhiza using site-specific *Alnus ncana* and *Melanogaster variegatus*s l.. Ecological Engineering, 57, 314-323.

Grey, D.H., Sotir, R.B., 1996.Biotechnical and soil bioengineering slope stabilization. In: A practical guide for erosion control. Willey, John & Sons, New York, pp. 1-105.

Han, L., Dutilleul, P., Prasher, S.O., Beaulieu, C., Smith, D.L., 2008. Assessment of common scab-induced pathogen effects onpotato underground organs via computed tomography scanning. Phytopathology, 98, 1118–1125.

742 Holzmann, H., Haselwandter, K., 1988. Contribution of nitrogen fixation to nitrogen
743 nutrition in an alpine sedge community (Caricetum curvulae). Oecologia, 76,
744 298-302. doi: 10.1007/BF00379967
745 Hu, X., Brierley, G., Zhu, H., Li, G., Fu, J., Mao, X., Yu, Q., Qiao, N., 2013. An
746 exploratory analysis of vegetation strategies to reduce shallow landslide activity
747 on loess hillslopes, Northeast Qinghai-Tibet Plateau, China. J. Mt. Sci., 10,
748 668–686.
749 Hu, X., Li, Z.C., Li, X.Y., Liu, L.Y., 2016. Quantification of soil macropores under
750 alpine vegetation using computed tomography in the Qinghai Lake Watershed,
751 NE Qinghai–Tibet Plateau. Geoderma, 264,244-251.
752 Hudek, C., Stanchi, S., D'Amico, M., Freppaz, M., 2017. Quantifying the contribution
753 of the root system of alpine vegetation in the soil aggregate stability of moraine.
754 International Soil and Water Conservation Research, 5, 36-42.
755 IBM Corp. Released 2013. IBM SPSS Statistics for Windows, Version 22.0. Armonk,
756 NY: IBM Corp.
757 Jenneson, P.M., Gilboy, W.B., Morton, E.J., Luggar, R.D., Gregory, P.J., Hutchinson,
758 D., 1999. Optimisation of X-ray microtomography for the in situ study of the
759 development of plant roots. 1999 Ieee Nuclear Science Symposium
760 Conference Record, 1–3, 429–432.
761 Jonasson, S., and Callaghan, T.V., 1992. Root Mechanical Properties Related to
762 Disturbed and Stressed Habitats in the Arctic. The New Phytologist 122, 179-
763 186.
764 Jones, G.A. and Henry, G.H.R., 2003. Primary plant succession on recently
765 deglaciated terrain in the Canadian High Arctic. Journal of Biogeography, 30,
766 277–296. doi:10.1046/j.1365-2699.2003.00818.x

767 Kaestner, A., Schneebeli, M., Graf, F., 2006. Visualizing three-dimensional root
768 networks using computed tomography. Geoderma, 136, 459–469.
769 Khan, M.A., Gemenet, D.C., Villordon, A., 2016. Root System Architecture and
770 Abiotic Stress Tolerance: Current Knowledge in Root and Tuber Crops. Front.
771 Plant Sci., 7, Article 1584.
772 Koebernick, N., Weller, U., Huber, K., Schlüter, S., Vogel, H.J., Jahn, R.,
773 Vereecken,H., Vetterlein, D., 2014. *In situ* visualization and quantification of
774 three-dimensional root system architecture and growth using x-ray computed
775 tomography. Vadose Zone, 13, 1-10.
776 Körner, C., 2003. Alpine plant life Functional plant ecology of high mountain
777 ecosystems. Springer-Verlag Berlin.
778 Kuka, K., Illerhaus, B., C.A., Fox, Joschko, M., 2013. X-ray Computed
779 Microtomography for the Study of the Soil–Root Relationship in Grassland
780 Soils. Vadose Zone Journal, 12, 1-10.
781 Lazzaro, A., Franchini, A.G., Brankatschk, R., Zeyer, J., 2010. Pioneer communities
782 in the forefields of retreating glaciers: how microbes adapt to a challenging
783 environment. In: Current Research, Technology and Education Topics in
784 Applied Microbiology and Microbial Biotechnology (Edi.Mendes-Villas, A.)
785 Formatex, Badajoz, Spain.
786 Lichtenegger, E., 1996. Root distribution in some alpine plants. Acta Phytogeogr.
787 Suec., 81, 76-82.
788 Lichtenegger, E., and Kutschera-Nitter, L., 1991. Spatial root types. In Edited by
789 McMichael, B.L., and Persson, H. Development in agricultural and managed
790 forests ecology 24. Plant roots and their environment. Proceedings of an ISRR
791 symposium Elsevier Science Publisher B.V. Amsterdam, Netherlands.

792 Lobet, G., Pound, M.P., Diener, J., Pradal, C., Drayer, X., Godin, C., Javaux, M.,
793 Leitner, D., Maunier, F., Nancy, P., Pridmore, T.P., Schnepf, A., 2015. Root
794 system markup language: toward a unified root architecture description
795 language. Plant Physiology, 167, 617-627.
796 Lontoc-Roy, M., Dutilleul, P., Prasher, S.O., Han, L., Brouillet, T., Smith, D.L., 2006.
797 Advances in the acquisition and analysis of CT scan data to isolate a crop root
798 system from the soil medium and quantify root system complexity in 3-Dspace.
799 Geoderma, 137, 231–241.
800 Mairhofer, S., Sturrock, C., Wells, D.M., Bennett, M.J., Mooney, S.J., Pridmore, T.P.,
801 2015. On the evaluation of methods for the recovery of plant root systems
802 from X-ray computed tomography images. Functional Plant Biology, 42, 460–
803 470.
804 Mairhofer, S., Zappala, S., Tracy, S.R., Sturrock, C., Bennett, M., Mooney, S.J.,
805 Pridmore, T., 2012. RooTrak: Automated Recovery of Three-Dimensional
806 Plant Root Architecture in Soil from X-Ray Microcomputed Tomography
807 Images Using Visual Tracking. Plant Physiology, 158, 561–569.
808 Massaccesi, L., Benucci, G.M.N., Gigliotti, G., Cocco, S., Corti, G., Agnelli, A., 2015.
809 Rhizosphere effect of three plant species of environment under periglacial
810 conditions (Majella massif, central Italy). Soil Biology and Biochemistry, 89,184-
811 195.
812 Matthews, J.A., 1999. Disturbance regimes and ecosystem response on recently-
813 deglaciated terrain. In Ecosystems of Disturbed Ground, Walker LR (ed.).
814 Elsevier: Amsterdam; 17–37.
815 Mercalli, L., 2003.Atlanteclimaticdella Valle d'Aosta. Societa Meteorologica Italia,
816 Torino 405.

817 Mooney, S.J., Morris, C., Berry, P.M., 2006. Visualization and quantification of the
818 effects of cereal root lodging on three-dimensional soil macrostructure using X-
819 ray Computed Tomography. Soil Sci, 171, 706–718.
820 Mooney, S.J., Pridmore, T.P., Helliwell, J., Bennett, M.J., 2012. Developing X-ray
821 Computed Tomography to non-invasively image 3-D root systems architecture
822 in soil. Plant Soil, 352, 1-22.
823 Nagel, K.A., Putz, A., Gilmer, F., Heinz, K., Fischbach, A., Pfeifer, J., Faget, M.,
824 Blossfeld, S., Ernst, M., Dimaki, C., Kastenholz, B., Kleinert, A.K., Galinski, A.,
825 Scharr, H., Fiorani, F., Schurr, U., 2012. GROWSCREEN-Rhizo is a novel
826 phenotyping robot enabling simultaneous measurements of root and shoot
827 growth for plants grown in soil-filled rhizotrons. Functional Plant Biology, 39,
828 891-904. http://dx.doi.org/10.1071/FP12023
829 Nagelmüller, S., Hiltbrunner, E., Körner, C., 2016. Critically low soil temperatures for
830 root growth and root morphology in three alpine plant species. Alp Botany
831 126, 11–21.
832 Norris, J.E., Stokes, A., Mickovski, S.B., Cammeraat, E., Van Beek, R., Nicoll, B.C.,
833 Achim, A., 2008. Slope stability and erosion control: ecotechnological
834 solutions. Springer, Dordrecht.
835 Ola, A., Dodd, I.C., Quinton, J.N., 2015. Can we manipulate root system architecture
836 to control soil erosion? SOIL, 1, 603-612.
837 Onipchenko, V.G., Kipkeev, A.M., Makarov, M.I., Kozhevnikova, A.D., Ivanov, V.B.,
838 Soudzilovskaia, N.A., Tekeev, D.K., Salpagarova, F.S., Werger, M.J.A.,
839 Cornelissen, J.H.C., 2014. Digging deep to open the white black box of snow
840 root phenology. Ecol Res, 29, 529–534.

841 Paez-Garcia, A., Motes, C.M., Scheible, W.-R., Chen, R., Blancaflor, E.B., Monteros,
842 M.J., 2015. Root Traits and Phenotyping Strategies for Plant
843 Improvement. Plants, 4, 334–355.
844 Paya, A.M., Silverberg, J., Padgett, J., Bauerle, T.L., 2015. X-ray computed
845 tomography uncovers root-root interactions: quantifying spatial relationships
846 between interacting root systems in three dimensions. Frontiers in Plant
847 Science, 6, 274.
848 Pérez-Harguindeguy, N., Díaz, S., Garnier, E., Lavorel, S., Poorter, H.,
849 Jaureguiberry, P., Bret-Harte, M.S., Cornwell, W.K., Craine, J.M., Gurvich,
850 D.E., Urcelay, C., Veneklaas, E.J., Reich, P.B., Poorter, L., Wright, I.J., Ray,
851 P., Enrico, L., Pausas, J.G., de Vos, A.C., Buchmann, N., Funes, G., Quétier,
852 F., Hodgson, J.G., Thompson, K., Morgan, H.D., ter Steege, H., van der
853 Heijden, M.G.A., Sack, L., Blonder, B., Poschlod, P., Vaieretti, M.V., Conti, G.,
854 Staver, A.C., Aquino S., Cornelissen, J.H.C., 2013. New handbook for
855 standardised measurement of plant functional traits worldwide. Australian
856 Journal of Botany, 61, 167–234.
857 Pierret, J.S., Prasher, S.O., Kantzas, A., Langford, C., 1999. Three-dimensional
858 quantification of macropore networks in undisturbed soil cores. Soil Sci. Soc.
859 Am. J, 63, 1530–1543.
860 Pierret, A., Moran, C., Doussan, C., 2005. Conventional detection methodology is
861 limiting our ability to understand the roles and functions of fine roots. New
862 Phytol, 166, 967–980.
863 Pignatti, S., 2003. Flora D'Italia. Vol.3. Edagricole S.r.l., Bologna.

Pfeifer, J., Kirchgessner, N., Colombi, T., Walter, A., 2015. Rapid phenotyping of crop root systems in undisturbed field soil using X-ray computed tomography. Plant Methods, 11, 41.

Pfeifer, J., Faget, M., Walter, A., Blossfeld, S., Fiorani, F., Schurr, U., Nagel, K.A., 2014. Spring barley shows dynamic compensatory root and shoot growth responses when exposed to localised soil compaction and fertilisation. Functional Plant Biology,41, 581-597.

Pohl, M., Alig, D., Körner, C., Rixen, C., 2009. Higher plant diversity enhances soil stability in disturbed alpine ecosystems. Plant Soil, 324, 91–102.

Pohl, M., Stroude, R., Buttler, A., Rixen, C., 2011. Functional traits and root morphology of alpine plants. Annals of Botany, 108, 537–545, doi:10.1093/aob/mcr169

Poorter, H., Niklas, K.J., Reich, P.B., Oleksyn, J., Poot, P., Mommer, L., 2012. Biomass allocation to leaves, stems and roots: meta-analyses of interspecific variation and environmental control. New Phytologist. 193, 30-50.

Reubens, B., Poesen, J., Danjon, F., Geudens, G., Muys, B., 2007. The role of fine and coarse roots in shallow slope stability and soil erosion control with a focus on root system architecture: a review. Trees, 21, 385–402.

Robbins, J.A., Matthews, J.A., 2009. Pioneer vegetation on glacier forefields in southern Norway: emerging communities? Journal of Vegetation Science, 20, 889-902.

Sati, S.P., Sundriyal, Y.P., 2007. Role of some species in slope instability. Himalayan Geol., 28, 75-78.

Siomos, M. F., 2009. Shaped by the environment – adaptation in plants. FEBS Journal, 276: 4705–4714. doi:10.1111/j.1742-4658.2009.07170.

889 Smith, S.E., Read, D.J., 2008. Mycorrhizal Symbiosis. Academic Press, Cambridge.
890 Soil Survay Staff, 2010. Keys to soil Taxonomy. United States Department of
891 Agriculture, Eleventh edition. Natural Resources Conservation Services.
892 Stokes, A., Atger, C., Bengough, A.G., Fourcaud, T., Sidle, R.C., 2009. Desirable
893 plant root traits for protecting natural and engineered slopes against landslides.
894 Plant Soil, 324, 1-30.
895 Stöcklin, J., Bäumler, E., 1996. Seed rain, seedling establishment and clonal growth
896 strategies on a glacier foreland. Journal of Vegetation Science., 9, 45-56.
897 Stöcklin, J., Kuss, P., Pluess, A.R., 2009. Genetic diversity, phenotypic variation and
898 local adaptation in the alpine landscape: case studies with alpine plant
899 species. Bot.Helv.119, 125-133.
900 Tasser, E., Tappeiner, U., 2005. New model to predict rooting in diverse plant
901 community compositions. Ecological Modelling, 185, 195-211.
902 Tisdall, J.M., 1991. Fungal hyphae and structural stability of soil. Australian Journal
903 of Soil Research, 29, 729-743.
904 Tollner, E.W., Rasmseur, E.L., Murphy, C., 1994.Techniquesand approaches for
905 documenting plant root development with X-ray computed tomography. In
906 Tomography of soil water-root processes. Edited by Anderson, S.H., and
907 Hopmans, J.W., SSSA Special Publication, 36, Madison,Wis. 115–133.
908 Tracy, S.R., Black, C.R., Roberts, J.A., Sturrock, C., Mairhofer, S., Craigon, J.,
909 Mooney, S.J., 2012. Quantifying the impact of soil compaction on root system
910 architecture in tomato (Solanum lycopersicum) by X-ray micro-computed
911 tomography. Ann. Bot., 110, 511-519.

912 Wantanabe, K., Mandang, T., Tojo, S., Ai, F., Huang, B.K., 1992. Non-destructive
913 root-zone analysis with X-ray CT scanner. Paper 923018. American Society of
914 Agricultural Engineers. St Joseph, MI, USA
915 Yang, Y., Chen, L., Li, N., & Zhang, Q., 2016. Effect of Root Moisture Content and Diameter
916 on Root Tensile Properties. *PLoS ONE*, *11*, e0151791.
917 Zoller, H., and Lenzin, H., 2006. Composed cushions and coexistence with
918 neighbouring species promoting the persistence of *Eritrichium nanum* in high
919 alpine vegetation. Bot. Helv., 116, 31–40.
920
921
922
923
924
925 **Table and Figure Captions**
926 **Table 1** The selected 10 pioneer plant species of the forefield of Lys Glacier
927 according to their Latin and common names, lifeforms, succession and family.
928
929 **Table 2** Scanning parameters for X-ray CT.
930
931 **Table 3** Values of root traits analyzed with RooTrak (volume, area, maximum vertical
932 and horizontal length of the root system, convex hull), ImageJ (maximum vertical and
933 horizontal length of the root system) and WinRHIZO (total root length and average
934 root diameter) of the X-ray CT scanned samples.
935

936 **Table 4** Plant height (mm), rooting depth (mm) measured with ImageJ, total root
937 length (m), mean root diameter (mm) and root length density (cm cm^{-3}) of the 10
938 studied alpine species measured with WinRHIZO.
939
940 **Table 5** Root length distribution (%) of the 10 pioneer alpine plants in relation to
941 different diameter classes (mm).
942
943 **Table 6** Life forms, the number of samples (n) tested, the range of root diameters
944 (mm), root tensile strength (MPa) values, scale factor (α) rate of strength decrease
945 (β) and the goodness of fit (R^2) of the 10 studied alpine species.
946
947 **Table 7** ANOVA table with multiple comparisons of root tensile strength (MPa)
948 between the studied plant species.
949
950 **Figure1 a - j** Root architecture of the 10 studied pioneer alpine species detected by
951 X-ray CT scanning. a., *E. fleischeri*; b., *F. halleri*; c., *L. alpine*; d., *L. spicata*; e., *M.*
952 *recurva*; f., *P. laxa*; g., *S. helvetica*; h., *S. exscapa*; i., *T. pallescens*; j., *T.*
953 *distichophyllum*; Scale bars: a., 35 mm, b., 25 mm, c., 40 mm, d., 15 mm, e., 10
954 mm, f., 15 mm, g., 15 mm, h., 30 mm, i., 45 mm, j., 20 mm.
955
956 **Figure 2** *a.,* Image of the core root system *b.,* the core root system in relation to the
957 soil matrix and *c.,* the washed entire root system of *Trifolium pallescens*. Scale bar
958 a., 45 mm b., 40 mm and c., the ruler uses cm.
959

960 **Figure 3** *a.,* Linear correlation between RooTrak and ImageJ data on the maximum
961 vertical and *b.,* horizontal root length for the 10 studied alpine species.
962
963 **Figure 4** Root length distribution (%) in relation to root diameter classes (mm) for the
964 10 studied alpine species
965
966 **Figure 5** Examples of the grayscale CT images of the soil matrices *a.,* glacial till with
967 *T. distichophyllum b.,* and *c.,* fluvio-glacial and lake depositions.
968
969 **Figure 6** Plant height (cm) and rooting depth (cm) of the 10 studied alpine plant
970 species.
971
972 **Figure 7** The relationship between root tensile strength (MPa) and root diameter
973 (mm) for the 10 studied alpine species.
974
975
976 **Table 1** The selected 10 pioneer plant species of the forefield of Lys Glacier
977 according to their Latin and common names, lifeforms, succession and family.
978

Species	Common name	Life form	Succession	Family
Epilobium fleischeri Hochst.	Alpine willowherb	Forb	Early	Omagraceae
Trisetum distichophyllum (Vill.) P.Beauve.	Tufted hairgrass	Graminoid	Early	Poaceae
Trifolium pallescens Schreb.	Pale clover	Forb	Early	Fabaceae
Luzula spicata (L.) DC.	Spiked woodrush	Graminoid	Mid	Juncaceae
Silene exscapa All.	Moss campion	Forb	Mid	Caryophyllaceae
Minuartia recurva (All.) Schinz and Thell.	Recurved sandwort	Forb	Late	Caryophyllaceae
Festuca halleri All.	Haller's Fescue	Graminoid	Late	Poaceae
Poa laxa Haenke	Banff Bluegrass	Graminoid	Ubiquitous	Poaceae
Salix helvetica Vill.	Swiss willow	Dwarf shrub	Ubiquitous	Salicaceae

Leucanthemopsis alpina (L.) Heyw.	Alpine Moon Daisy	Forb	Ubiquitous	Asteraceae

Table 2 Scanning parameters for X-ray CT.

Voltage (kV)	Current (µA)	Number of projections	Exposure time (ms)	Resolution (µm)	Signal averaging	Total scanning time
180	160	2160	250	54	4/1	2h17min

Table 3 Values of root traits analyzed with RooTrak (volume, area, maximum vertical and horizontal length of the root system, convex hull), ImageJ (maximum vertical and horizontal length of the root system) and WinRHIZO (total root length and average root diameter) of the X-ray CT scanned samples.

Commented [SS4]: Pls set horizontal

Plant species	Root type	RooTrak					ImageJ		WinRHIZO		
		Volume (mm^3) (total mass of the root system)	Area (mm^2) (root area in direct contact with the soil)	Depth (mm) (root system's maximum vertical distance)	Width (mm) (root system's maximum horizontal distance)	Convex hull (mm^2) (region of soil explored by the root system)	Vertical length (mm)	Horizontal length (mm)	Total root length (m) (roots 1-5 mm in diameter)	Total root length (m) (roots 0.1-0.5 mm in diameter)	Average root diameter (roots 0.1-0.5 mm in diameter)
T. distichophyllum	Cylindrical	353	3399	63	68	65774	75	70	1.81	192.7	0.21
E. fleischeri	Pole	967	3711	105	65	90931	115	70	0.05	59.2	0.17
T. pallescens	Cone↑	1530	7752	132	72	505364	225	70	1.97	51.6	0.30
S. exscapa	Cone↑	385	2383	102	70	357053	173	69	1.84	95.3	0.24
L. spicata	Cone↓	306	2106	39	71	27046	137	70	1.60	100.3	0.16
F. halleri	Cone↓	828	5866	67	71	60318	107	55	0.65	20.7	0.31
M. recurva	Discoid	144	1677	44	68	60237	164	50	1.96	50.5	0.29
P. laxa	Cone↓	150	1547	33	72	45612	119	34	0.22	10.5	0.26
L. alpina	Umbrella	542	4666	126	72	224012	141	69	1.06	62.2	0.26
S. helvetica	Discoid	435	1146	35	73	24117	49	39	1.90	56.5	0.28

Table 4 Plant height (mm), rooting depth (mm) measured with ImageJ, total root length (m), mean root diameter (mm) and root length density (cm cm^{-3}) of the 10 studied alpine species measured with WinRHIZO.

Plant species	Plant height (mm)	Rooting depth (mm)	Total root length (m)	Mean root diameter (mm)	Root length density (cm cm^{-3})
T. distichophyllum	50	133	336.9	0.21	85
E. fleischeri	65	197	75.3	0.23	9
T. pallescens	47	133	197.6	0.47	33
S. exscapa	20	153	106.2	0.33	49
L. spicata	30	117	202.1	0.22	81
F. halleri	32	101	297.8	0.35	59

M. recurva	15	118	135.9	0.32	29
P. laxa	51	119	210.1	0.28	47
L. alpina	20	127	368.5	0.26	53
S. helvetica	25	90	342.3	0.27	68

Table 5 Root length distribution (%) of the 10 pioneer alpine plants in relation to different diameter classes (mm).

	0<L<0.1	**0.1<L<0.2**	**0.2<L<0.3**	**0.3<L<0.4**	**0.4<L<0.5**	**0.5<L<0.75**	**0.75<L<1**	**1<L<1.5**	**1.5<L<2**	**2<L<5**
T. distichophyllum	33	41	15	5	2	1	1	0	0	0
T. pallescens	49	19	10	5	4	6	2	2	1	1
S. exscapa	42	30	12	5	3	4	2	2	0	0
L. spicata	57	27	9	3	1	1	0	0	0	0
F. halleri	37	22	15	8	5	7	3	2	1	0
M. recurva	36	30	13	6	3	5	3	3	1	0
P. laxa	49	19	12	6	4	5	3	2	0	0
L. alpina	36	29	14	7	5	5	2	1	0	0
S. helvetica	9	25	37	6	4	4	1	2	3	9

Table 6 Life forms, the number of samples (n) tested, the range of root diameters (mm), root tensile strength (MPa) values, scale factor (α) rate of strength decrease (β) and the goodness of fit (R^2) of the 10 studied alpine species.

Species	Life form	n	*d* range (mm)	Mean Tr (MPa)	α	β	R^2	p
T. distichophyllum	Graminoid	30	0.05-1.15	86	23.26	0.62	0.56	<0.001
E. fleischeri	Forb	32	0.04-1.56	58	3.61	1.15	0.67	<0.001
T. pallescens	Forb	32	0.05-1.66	44	10.55	0.88	0.65	<0.001
S. exscapa	Forb	30	0.03-1.14	54	11.85	0.84	0.65	<0.001
L. spicata	Graminoid	30	0.03-0.37	138	9.54	1.01	0.71	<0.001
F. halleri	Graminoid	30	0.05-0.46	94	17.92	0.75	0.70	<0.001
M. recurva	Forb	30	0.03-0.35	60	6.24	1.11	0.78	<0.001
P. laxa	Graminoid	30	0.03-0.56	113	21.65	0.75	0.82	<0.001
L. alpina	Forb	32	0.05-0.59	29	8.67	0.75	0.71	<0.001
S. helvetica	Dwarf shrub	30	0.03-0.78	110	11.34	0.94	0.78	<0.001

Table 7 ANOVA table with multiple comparisons of root tensile strength (MPa) between the studied plant species.

Figure1 a - j Root architecture of the 10 studied pioneer alpine species detected by X-ray CT scanning. a., *E. fleischeri*; b., *F. halleri*; c., *L. alpine*; d., *L. spicata*; e., *M. recurva*; f., *P. laxa*; g., *S. helvetica*; h., *S. exscapa*; i., *T. pallescens*; j., *T.*

distichophyllum; Scale bars: a., 35 mm, b., 25 mm, c., 40 mm, d., 15 mm, e., 10 mm, f., 15 mm, g., 15 mm, h., 30 mm, i., 45 mm, j., 20 mm.

a., *E. fleischeri* b., *F. halleri*

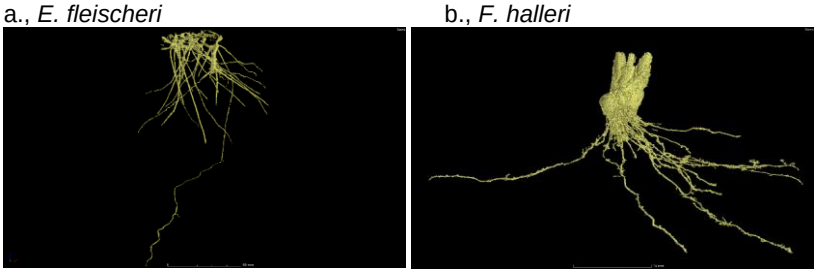

c., *L. alpina* d., *L. spicata*

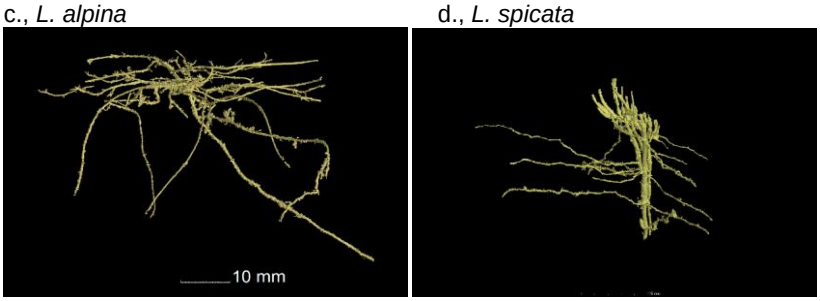

e., *M. recurva* f., *P. laxa*

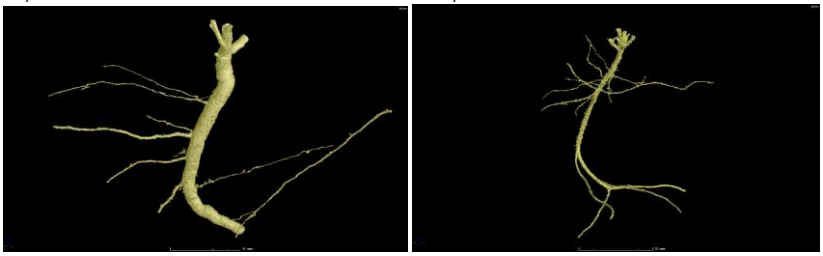

g., *S. helvetica* h., *S. exscapa*

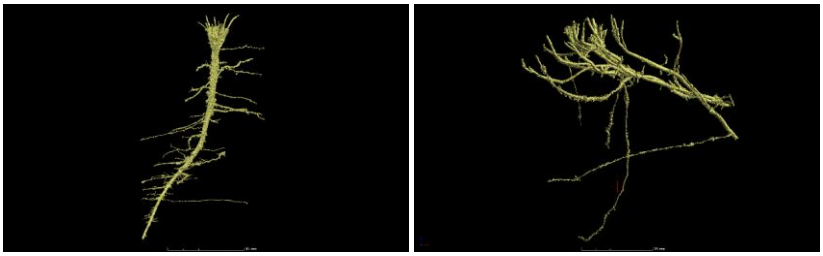

i., *T. pallescens* j., *T. distichophyllum*

Figure 2 *a.,* Image of the cored root system *b.,* the core root system in relation to the soil matrix and *c.,* the washed entire root system of *Trifolium pallescens*. Scale bar a., 45 mm b., 40 mm and c., the ruler uses cm.

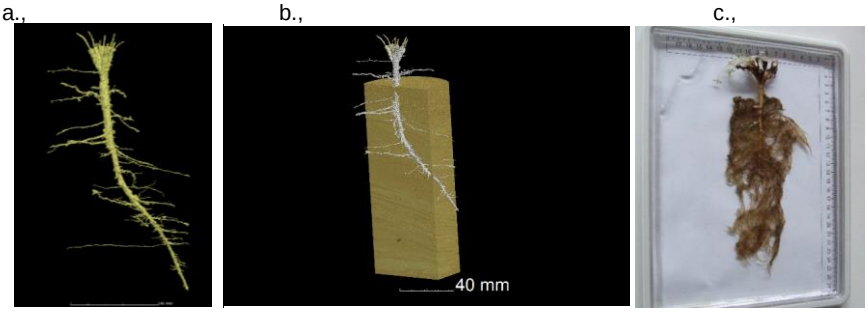

Figure 3 *a.,* Linear relationship between RooTrak and ImageJ data on the maximum vertical and *b.,* horizontal root length for the 10 studied alpine species.

Commented [SS5]: I would prefer c orrelation to regression. Make univoque text and fugure. If you keep the text (correlation) delete R2 from figure 3

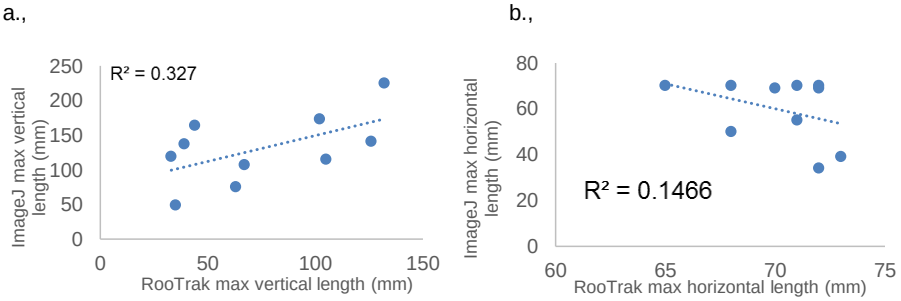

Figure 4 Root length distribution (%) in relation to root diameter classes (mm) for the 10 studied alpine species

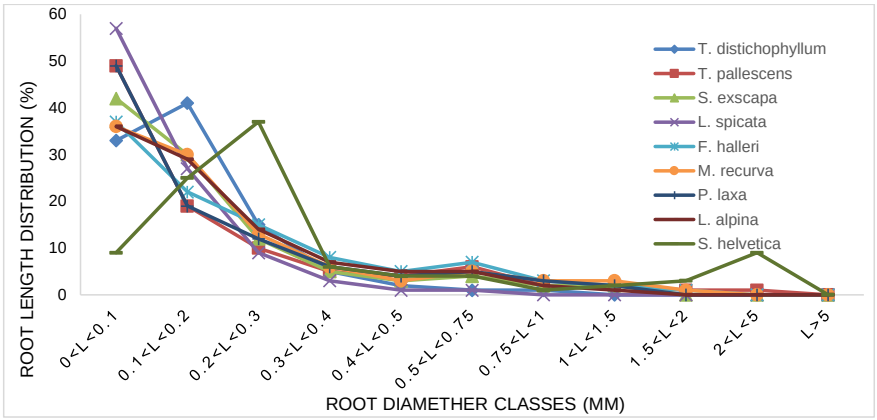

Figure 5 Examples of the grayscale CT images of the soil matrices *a.,* glacial till with *T. distichophyllum b.,* and *c.,* fluvio-glacial and lake depositions.

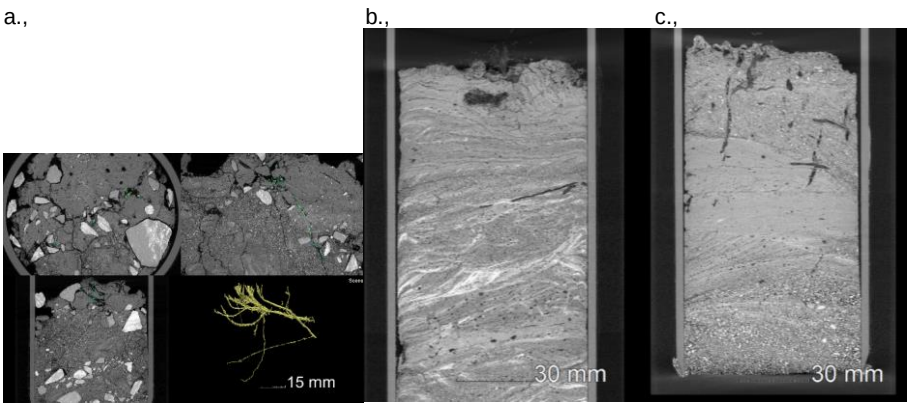

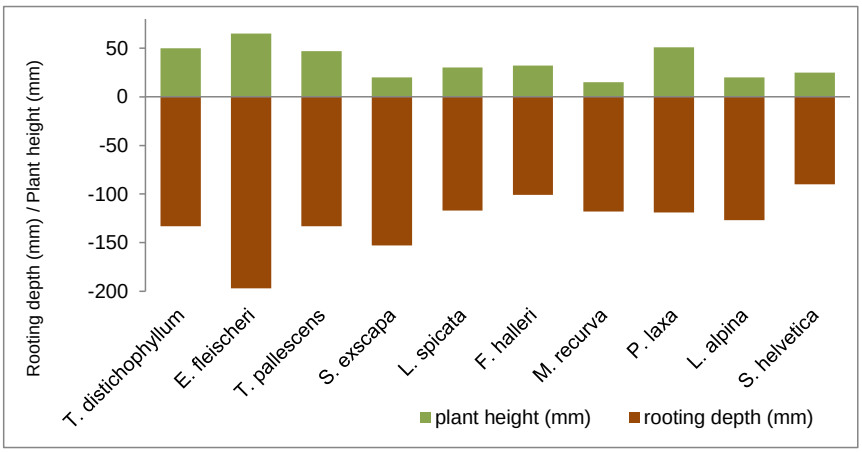

1041 **Figure 6** Plant height (cm) and rooting depth (cm) of the 10 studied alpine plant species.

1042

1043

1044

1045

1046 **Figure 7** The relationship between root tensile strength (MPa) and root diameter

1047 (mm) for the 10 studied alpine species

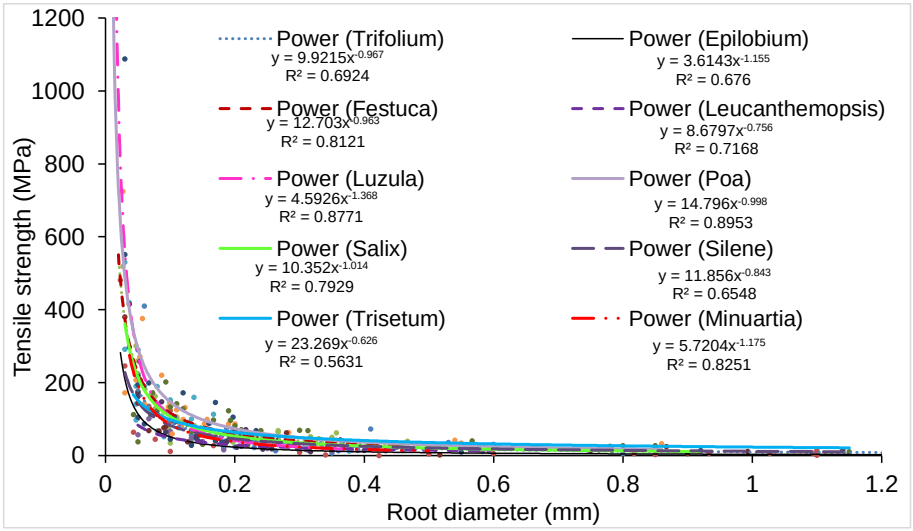

1048

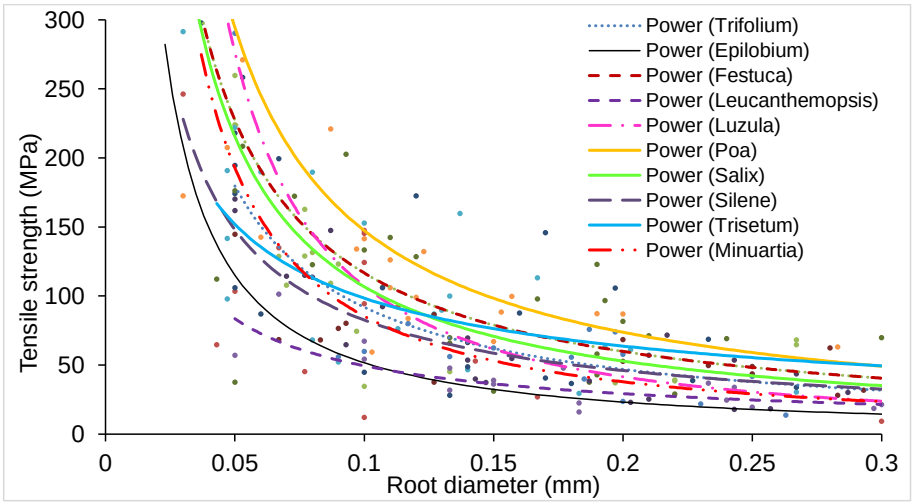
Tensile strength (MPa)
300
250
200
150
100
50
0
0
0.05
0.1
0.15
0.2
0.25
0.3
Root diameter (mm)
Power (Trifolium)
Power (Epilobium)
Power (Festuca)
Power (Leucanthemopsis)
Power (Luzula)
Power (Poa)
Power (Salix)
Power (Silene)
Power (Trisetum)
Power (Minuartia)

1049